660 nm LED Light Irradiation Promotes the Healing of the Donor Wound of Free Gingival Graft

Chen-Ying Wang[*], Sheng-Chueh Tsai[†], Min-Chen Yu[*‡], Yu-Fang Lin[§], Chih-Cheng Chen[§], Po-Chun Chang[*‡]

[*] Department of Dentistry, National Taiwan University Hospital, Taipei, Taiwan.

† Institute of Molecular and Cellular Biology, College of Life Science, National Taiwan University, Taipei, Taiwan.

‡ Graduate Institute of Clinical Dentistry, School of Dentistry, National Taiwan University, Taipei, Taiwan.

§ Taiwan Mouse Clinics-National Phenotyping and Drug Testing Center, National Research Program for Biopharmaceuticals, National Science Council, Taipei, Taiwan.

Background: This study aimed to evaluate the effect of the light-emitting diode (LED) light irradiation on the donor wound of free gingival graft.

Materials and Methods: Rat gingival fibroblasts were chosen to assess the cellular activities and *in vitro* wound healing under 0-20 J/cm^2 LED light irradiation. Seventy-two Sprague-Dawley rats received daily 0, 10 (low-dose; LD), 20 (high-dose; HD) J/cm^2 LED light irradiation on the opened palatal wound respectively and were euthanized after 4-28 days; the healing pattern was assessed by histology, histochemistry for collagen deposition, and immunohistochemistry for tumor necrosis factor-alpha (TNF-α) infiltration. We also evaluated the wound mRNA levels of heme oxygenase-1 (HO-1), TNF-α, the receptor for advanced glycation end-products (RAGE), vasculo-endothelial growth factor (VEGF), periostin, type I collagen, and fibronectin.

Results: Cellular viability and wound closure were significantly promoted and cytotoxicity was significantly inhibited under 5 J/cm^2 LED light irradiation *in vitro*. The wound closure, re-epithelialization, and collagen deposition were accelerated, and sequestrum formation, and inflammatory cell and TNF-α infiltration, was significantly reduced in the LD group. HO-1 and TNF-α were significantly up-regulated in the HD group, and most of the repair-associated genes were significantly up-regulated in both the LD and HD groups at day 7. Persistent RAGE up-regulation was noted in both the LD and HD groups until day 14.

Conclusion: 660 nm LED light irradiation accelerated palatal wound healing, potentially via reducing reactive oxygen species production, facilitating angiogenesis, and promoting provisional matrix and wound reorganization.

KEYWORDS:

periodontal tissue; wound healing; histology; laser therapy, lower level; transplant

In order to restore the mucogingival deformity of the dentalveolar apparatus, a variety of surgical techniques, including free gingival graft (FGG) [1], subepithelial connective tissue graft [2], allogenic

dermal matrix [3], and even a tissue engineering construct with allogenic cells [4], have been developed to increase the keratinized gingiva. The FGG, one of the most classic approaches developed a half century ago, remains the gold standard because of the high success and predictability [4]. However, the major complication of FGG is the post-operative morbidity associated with the open palatal wound, including acute pain, excessive hemorrhage, and bone exposure [5]; these complications are not resolved until the completion of wound epithelialization, which usually takes 2-4 weeks [6]. To accelerate the healing process and to reduce the incidence of complications, chemotherapeutic agents, including antibiotics and mouthrinse [7], hemostatic agents [8], ozonides [9], and low-intensity pulse ultrasound [10] were introduced.

Recently, lower-level laser therapy (LLLT) was utilized to accelerate wound healing. LLLT is defined as the light source with an energy density below 100 J/cm^2; therefore, the temperature change can be neglected to minimize tissue damage [11]. By activating mitochondrial photoacceptor molecule cytochrome *c* oxidase [12], LLLT can enhance coagulation [13], angiogenesis [14], collagen deposition [15], and fibroblastic proliferation [16]. Recently, Firat and co-workers showed the potential of LLLT application for promoting palatal wound healing by irradiating with a 10 J/cm^2 GaAlAs laser and reported that the healing of palatal mucoperiosteal wounds was promoted, which was presumably associated with increasing the mitogenesis of fibroblasts [17].

Compared to lasers, by providing similar wavelengths and light energy, the light-emitting diode (LED) has demonstrated comparable biological effects [18] and is an economical alternative to lasers. As our group has recently reported, the adjunctive effect of 660-nm LED light facilitates tissue recovery from experimental periodontitis [19]. In the present study, we aimed to further evaluate the potential application of 660 nm LED light on the healing of the donor wound of FGG. After a preliminary *in vitro* examination of the LED light effect on the gingival fibroblasts was done, a rodent model was utilized to investigate the healing of a palatal mucosal wound under the LED light irradiation, and the gene expression profile in the wound was examined to evaluate the potential mechanism *in vivo*.

MATERIALS AND METHODS

LED Device

Light-emitting diode (LED) light irradiation was delivered by directly emitting 660±25 nm and 3.5 mW/cm^2 of visible red light‖ on the culture plates or gingival wound to achieve an energy density of 5, 10, or 20 J/cm^2 (6, 12, or 24 minutes of irradiation) within the tested region, as previously described [19].

In Vitro Study Design and Assessments

Gingival fibroblasts (GFs) were harvested from the palatal mucosa of rats during the preparation of the palatal wounds described below. After dissecting the tissue, the fragments were placed in dishes

containing Dulbecco's modified Eagle's growth medium supplemented with 10% fetal bovine serum, 100 U/mL penicillin and 100 mg/ml streptomycin. GFs migrated from the border of fragments 5 days later, and after 3-4 passages, GFs were isolated and cultured at a density of $4x10^3$ cells/well in 96-well plates for mitogenesis and cytotoxicity, and they were given daily 0, 5, 10, or 20 J/cm^2 LED light irradiations for 24 and 72 hours. Cellular viability was evaluated with a cell proliferation assay[¶]. Cytotoxicity was evaluated using a cytotoxicity detection kit[#]. Wound closure was evaluated using a scratch wound created by a 200 μl pipette tip [20] at the density of $1.2x10^5$ cells/well in 12-well plates, and the images were acquired at 40x using a digital image acquisition system[**]. Specimens were evaluated 6 and 12 hours after we administered 0, 5, 10, or 20 J/cm^2 LED light irradiations. All *in vitro* experiments were performed in triplicate.

Animal Model

All procedures performed on animals followed the approved protocol no. 20130054 from the Institutional Animal Care and Use Committee of the National Taiwan University. A total of 72 male Sprague-Dawley rats (250-300 gm) were utilized. In each rat, bilateral 5x1.5 mm^2 palatal wounds parallel to the gingival margin of maxillary molars with 1 mm distance were created using a double-bladed scalpel (1.5 mm inter-blade distance) with two No. 15 surgical blades as previously described [21], and the LED light irradiation was started immediately after the wound creation. Animals were equally divided into three groups, including the control group (Ctrl group, no LED light irradiation), the low-dose group (LD group, daily 10 J/cm^2 LED light irradiation), and the high-dose group (HD group, daily 20 J/cm^2 LED light irradiation). Equal numbers of animals were euthanized after 4, 7, 14, and 28 days of LED treatment (n=6/group/time point), and bilateral maxillae were harvested. Tissue within the palatal wound in one randomly-selected side of the maxillae was excised to evaluate the gene expression levels, and the other side of the maxillae was fixed in10% formaldehyde for histological examination.

Histological Examinations

After fixation, the maxillae were decalcified with 12.5% ethylenediaminetetraacetic acid and embedded in paraffin. Sections (5 μm) from the cross-sectional plane at the mid-wound area were selected, and one was stained with hematoxylin and eosin, one was stained with Masson's trichrome for the assessment of collagen deposition, and the other one was stained immunohistochemically using a commercialized staining kit[††] with a polyclonal anti-TNF-α antibody[‡‡] (dilution 1:200). All of the images were acquired using a digital image acquisition system[§§].

Wound healing was assessed by the fraction of inflammatory cells/total cells, status of re-epithelialization and wound closure, scar elevation index (SEI, an index to express the degree of scar hypertrophy in the healing process [22]), the fraction of collagen deposition/lamina propria, and the fraction of TNF-α-positive area/lamina propria, were evaluated using an image analysis software[‖‖] as previously described [21], and the definitions of the parameters are listed in the supplementary

appendix in the online *Journal of Periodontology*. A blinded examiner performed and averaged all measurements from three consecutive slides of the same staining protocol.

Real-Time PCR Analysis

The RNA harvested from the tissue was reverse transcribed to cDNA utilizing a cDNA synthesis kit[¶¶], and the mRNA levels of genes were quantitatively analyzed with a real-time PCR system[##] and sequence-specific TaqMan gene expression assays[***] for GAPDH (housekeeping gene), heme oxygenase-1 (HO-1, marker of dissociating reactive oxygen species (ROS) [23]), receptor for advanced glycation end-products (RAGE), TNF-α, fibronectin (extracellular matrix protein for cell attachment), periostin (matricellular protein essential for periodontal tissue integrity [24]), and type I collagen (major extracellular matrix protein in the periodontium). The gene expression levels were normalized to GAPDH, and data are presented as the relative expression to the averaged levels of the non-LED treated specimens of the same time point. All experiments were performed in triplicate.

Statistical Analysis

The sample size was determined by the Power Analysis based on the results from our previous study and under the assumption of 80% power, α=0.05, and normal distribution and equivalent variance of the samples [21]. Two-way ANOVA followed by Bonferroni post-tests were used to compare the difference between the control and LED light-irradiated groups at each time point. The data are presented as the mean ± standard deviation of the measurements, and a *p*-value less than 0.05 was considered statistically significant.

RESULTS

In Vitro Assessments

Cellular viability was significantly promoted in the specimens treated with 5 ($p<0.001$) and 20 ($p<0.05$) J/cm^2 LED lights at 72 hours (Figure 1A). Cytotoxicity was generally reduced under LED irradiation, and a significant difference compared to the non-irradiated control was noted in 5 J/cm^2 LED-irradiated specimens at 24 ($p<0.05$) and 72 ($p<0.01$) hours (Figure 1B). However, wound closure was significantly promoted under 5 J/cm^2 LED irradiation at 12 hours (Figure 1C).

Descriptive Histology

At day 4, the underlying alveolar bone was exposed and partially covered by a necrotic tissue mass, aggregated erythrocytes, and inflammatory cells in all groups (data not shown). Epithelium approximation was noted in all groups at day 7, and the wound mostly consisted of inflammatory cells and primitive fiber matrix, and sequestrum was noted in most specimens (Figure 2A-C). The wound was nearly completely covered by the epithelium without prominent rete pegs, and hypertrophy of the connective tissue matrix was noted in most specimens at day 14 (Figure 2D-F). Inflammatory cells and the degraded collagen matrix were surrounded by sequestrum, and

sequestrum was engaged with down-grown epithelium in 4 of 6 specimens in the Ctrl and HD groups, and the sequestrum was apparently smaller in the HD group (Figure 2D and 2F). There was no sequestrum with a reduced inflammatory level in 5 of 6 specimens in the LD group (Figure 2C). The sequestrum was clear in all LED-irradiated specimens at day 28, whereas sequestrum still presented in 4 of 6 specimens in the Ctrl group (Figure 2G-I). Inflammation was subsided in the lamina propria of most specimens, and the extension of rete pegs was noted in the Ctrl and LD groups (Figure 2G-H).

Collagen Matrix Deposition and TNF-α Infiltration

The collagen fibril matrix deposition was initiated after 7 days of wound creation in all groups (Figure 3A) and gradually deposited and aligned within the cervical part of lamina propria of the Ctrl and HD groups at day 14 (Figure 3B). In the LD group, the lamina propria was nearly occupied with aligned collagen fibril matrix at day 14 (Figure 3C), and the fibril bundles were apparently more densely packed at day 28 (Figure 3D).

At day 7, TNF-α was widely-distributed on the edge of sequestrum and the necrotic tissue mass in the Ctrl group (Figure 3E), whereas the TNF-α-positive area was relatively small in the LD and HD groups (Figure 3F). TNF-α became restricted to the edge of sequestrum and epithelial approximation in the Ctrl and HD groups at day 14 (Figure 3G). Without the presence of sequestrum, TNF-α was scattered and lightly distributed in the collagen matrix in the LD group from day 14 and in the HD group from day 28 (Figure 3H). However, TNF-α infiltration was still evident on the edge of sequestrum in the Ctrl group at day 28 (Figure 3I).

Quantitative Histologic Assessments

The wound closure and re-epithelialization were apparently accelerated in both the HD and LD groups relative to the Ctrl group at day 7, and the difference was less among groups at the later stages (Figure 4A-B). The SEI was increased in the LED light-irradiated groups at day 7, and a significant difference compared to the Ctrl group was noted in the HD group ($p<0.05$, Figure 4C). The lamina propria was hypertrophic at day 14, but it recessed at day 28, without an obvious difference between groups. Inflammatory cell infiltration was gradually reduced in the Ctrl group from day 7 to 28, and the level was consistently significantly lower in the LD group (Figure 4D). Collagen deposition was dramatically increased at day 14 in all groups. The deposition was consistently higher in the LD and HD groups at days 14 and 28 (Figure 4E), and the LD group was significantly different compared to the Ctrl group at both time points ($p<0.01$, Figure 4E). The TNF-α-positive area was gradually reduced in all groups from day 7 to 28 and consistently smaller in the LD and HD groups (Figure 4F), and significantly smaller TNF-α-positive area relative to the Ctrl group was noted in the LD group at days 7 and 14 ($p<0.05$, Figure 4F).

Gene Expression Profiles

HO-1 expression was up-regulated in the HD group until day 14 (Figure 5A), with a significant difference compared to the control and LD groups at day 7 ($p<0.001$) and compared to the Ctrl group at day 14 ($p<0.05$). TNF-α was up-regulated in the LD and HD groups in the first 7 days (Figure 5B), and significant up-regulation compared to the Ctrl group was noted in the HD group on day 4 ($p<0.001$). Therefore, RAGE was significantly up-regulated in the LD and HD groups at day 7 ($p<0.05$ and $p<0.01$, Figure 5C), and the most significant difference compared to the Ctrl group was noted at day 14 ($p<0.001$ in both groups). At day 28, the significant difference, compared to the Ctrl group, was still observed in the HD group ($p<0.01$).

The expression profiles of VEGF, periostin, fibronectin, and type I collagen were generally similar (Figure 5D-G). At day 4, there was slightly but insignificantly increased expression of these genes compared to the Ctrl group in the HD group. However, at day 7, significant up-regulation of these genes was noted in the LD and HD groups ($p<0.001$), whereas the levels of periostin and type I collagen were significantly higher in the HD group compared to those of the LD group ($p<0.001$). On days 14 and 28, there were no significant differences in gene expression among the groups.

DISCUSSIONS

Opened palatal wound healing involves a dynamic series of processes, including blood clot deposition, inflammation, and angiogenesis, to form a vascularized granulation tissue, which is followed by an approximation of epithelium and tissue remodeling to achieve a mature healing status in 4 weeks [25, 26]. It is generally accepted that LLLT facilitates wound healing by altering the cellular behavior of fibroblasts and keratinocytes [27], enhancing collagen synthesis [28], angiogenesis and growth factor release [29, 30], and the effect of LLLT irradiation is dose-dependent [31, 32]. As an alternative source of LLLT, the results from the present study showed that the proliferation of the gingival fibroblasts was significantly promoted, accompanying with significantly inhibited cytotoxicity and significantly accelerated *in vitro* wound closure under 5 J/cm^2 LED light irradiation (Figure 1). With the implementation of 10 or 20 J/cm^2 LED light on the palatal wound, wound closure and re-epithelization were accelerated, and there was apparent, rapid recovery from scar hypertrophy, reduced inflammatory cell infiltration and sequestrum, and collagen deposition promotion (Figures 2-4). These findings are in agreement with previous studies [19, 33] and support LED light as favorable in facilitating palatal wound healing.

The underlying mechanism of LED light-aided wound healing was examined by the gene expression profile. LED light irradiation may directly dissociate reactive oxygen species (ROS) to prevent cell injury [34], and with the reduction of ROS, HO-1 was up-regulated [23], subsequently promoting neovascularization by stimulating VEGF production [35]. We found that both HO-1 and VEGF were up-regulated in the LD and HD groups within 7 days (Figures 5A and 5D) and supported that LED light attenuated the deleterious effect of ROS and promoted angiogenesis in the

early healing stage. Additionally, genes associated with tissue repair and homeostasis, including fibronectin, type I collagen, and periostin, were up-regulated in both the LD and HD groups at day 7 (Figures 5E-G). Fibronectin serves as a chemotactic factor of epidermal keratinocytes and is required for assembling type I collagen, the major component of the extracellular matrix [36]. Periostin was reported to increase the cross-linking of collagen matrix and maintain matrix integrity [24]. These results seem to indicate that LED light irradiation facilitates both the deposition of the provisional matrix and the reorganization of the connective tissues. Consequently, both re-epithelization and recovery from scar hypertrophy were accelerated in the present study (Figures 4B-C).

LLLT had been reported to eliminate the symptoms and prevent bone exposure in the patients with bisphosphonates-related osteonecrosis of the jaws [37, 38], and the results from our study showed that sequestrum formation was reduced with the LED light irradiation, especially in the LD group (Figure 2), supporting that LED light may exhibit similar but dose-dependent effect in preventing osteonecrosis as LLLT. The reduction of sequstrum formation appeared to be parallel to the reduction of inflammatory cell infiltration and TNF-α infiltration (Figures 3, 4D, and 4F). However, the expression of TNF-α was temporarily up-regulated in the HD group (Figure 5B). It is noteworthy that LED light may also activate immune cell activity [39] such that the up-regulation of inflammation-associated genes in the wound might not be preventable. Therefore, the inflammatory cell as well as TNF-α infiltration was still reduced, and collagen deposition was slightly accelerated relative to the Ctrl group (Figures 4D-F), suggesting that the up-regulation of the inflammatory signaling in the HD group did not significantly retard the healing process. Furthermore, RAGE was up-regulated with the LED light irradiation from day 7 (Figure 5C). RAGE has been recognized as a key molecule to committed inflammation and also serve as a precursor to attenuate acute inflammation and promote chemotaxis in repairing tissue [40]. According to the reduction of inflammation and promotion of collagen deposition in the LD and HD groups (Figures 4D-F), the up-regulation of RAGE signaling might associate with the remission of the tissue repair. Further investigations on the entire profile of proinflammatory cytokines and RAGE signaling on the healing wound will be required.

It appeared that the biomodulation of LED light irradiation was attenuate after 14 days, whereby no significant difference between the LED and non-LED light-irradiated groups was noted in any histological parameter or examined gene (Figures 4 and 5). As complete wound closure without significant scar elevation was noted in several non-LED light irradiated specimens (Figures 4A and 4C), this palatal wound was not considered as a critical-sized defect. However, the critical-sized palatal wound resembling the donor wound of FGG might not be achievable in the rats due to the limited dimension of the palate. On the other hand, the newly-formed tissue in the wound was too small to confirm the titers of other proinflammatory cytokines, especially in the early healing stages. In this respect, it is difficult to confirm the influence of the up-regulation of inflammatory signaling under LED light irradiation. Nevertheless, a partial-thickness flap was not technically achievable in the rat palate, and the exposure of the underlying bone might increase the incidence of wound morbidity. Furthermore, the healing capability of animals might not be relevant to humans, and the

rationalization of the LED light condition for human use is still controversial. Future studies to justify the indications and conditions of LED light for human use are still needed.

CONCLUSION

Notwithstanding the limitations of the study, we conclude that 660 nm LED light irradiation, specifically within 10-20 J/cm^2 energy density, facilitates the healing of opened palatal wounds, potentially via reducing ROS production and angiogenesis and by promoting provisional matrix and tissue reorganization *in vivo*. Further justifications of the LED light and experimental models as well as the investigations of the inflammation profiles and RAGE signaling are warranted.

ACKNOWLEDGEMENTS

The authors acknowledge the technical support from the Pathology Department of National Taiwan University Hospital. The study was supported by the research grants 101R7465 from the National Taiwan University, 102-M2301 and 103-M2577 from the National Taiwan University Hospital, and 103-2314-B-002-095-MY2 from the Ministry of Science and Technology (Taiwan). The authors declare no conflicts of interest related to the study.

CONFLICT OF INTEREST AND SOURCE OF FUNDING STATEMENT

The study was supported by the research grants 101R7465 from the National Taiwan University, 102-M2301 and 103-M2577 from the National Taiwan University Hospital, and 103-2314-B-002-095-MY2 from the Ministry of Science and Technology (Taiwan). The authors declare no conflicts of interest related to the study.

REFERENCES

1. Nabers JM. Free gingival grafts. *Periodontics* 1966;4:243-245.
2. Lee YM, Kim JY, Seol YJ, et al. A 3-year longitudinal evaluation of subpedicle free connective tissue graft for gingival recession coverage. *J Periodontol* 2002;73:1412-1418.
3. de Queiroz Cortes A, Sallum AW, Casati MZ, Nociti FH, Jr., Sallum EA. A two-year prospective study of coronally positioned flap with or without acellular dermal matrix graft. *J Clin Periodontol* 2006;33:683-689.
4. McGuire MK, Scheyer ET, Nunn ME, Lavin PT. A pilot study to evaluate a tissue-engineered bilayered cell therapy as an alternative to tissue from the palate. *J Periodontol* 2008;79:1847-1856.
5. Griffin TJ, Cheung WS, Zavras AI, Damoulis PD. Postoperative complications following gingival augmentation procedures. *J Periodontol* 2006;77:2070-2079.
6. Silva CO, Ribeiro Edel P, Sallum AW, Tatakis DN. Free gingival grafts: graft shrinkage and donor-site healing in smokers and non-smokers. *J Periodontol* 2010;81:692-701.
7. Kaigler D, Avila G, Wisner-Lynch L, et al. Platelet-derived growth factor applications in periodontal and peri-implant bone regeneration. *Expert Opin Biol Ther* 2011;11:375-385.

8. Rossmann JA, Rees TD. A comparative evaluation of hemostatic agents in the management of soft tissue graft donor site bleeding. *J Periodontol* 1999;70:1369-1375.

9. Patel PV, Kumar S, Vidya GD, Patel A, Holmes JC, Kumar V. Cytological assessment of healing palatal donor site wounds and grafted gingival wounds after application of ozonated oil: an eighteen-month randomized controlled clinical trial. *Acta Cytologica* 2012;56:277-284.

10. Maeda T, Masaki C, Kanao M, et al. Low-intensity pulsed ultrasound enhances palatal mucosa wound healing in rats. *J Prosthodont Res* 2013;57:93-98.

11. Conlan MJ, Rapley JW, Cobb CM. Biostimulation of wound healing by low-energy laser irradiation. A review. *J Clin Periodontol* 1996;23:492-496.

12. Eells JT, Wong-Riley MT, VerHoeve J, et al. Mitochondrial signal transduction in accelerated wound and retinal healing by near-infrared light therapy. *Mitochondrion* 2004;4:559-567.

13. Hoffman M, Monroe DM. Low intensity laser therapy speeds wound healing in hemophilia by enhancing platelet procoagulant activity. *Wound Repair Regen* 2012;20:770-777.

14. Lim WB, Kim JS, Ko YJ, et al. Effects of 635nm light-emitting diode irradiation on angiogenesis in CoCl(2) -exposed HUVECs. *Lasers Surg Med* 2011;43:344-352.

15. Grandin HM, Gemperli AC, Dard M. Enamel matrix derivative: a review of cellular effects in vitro and a model of molecular arrangement and functioning. *Tissue Eng Part B Rev* 2012;18:181-202.

16. Oliveira Sampaio SC, de CMJS, Cangussu MC, et al. Effect of laser and LED phototherapies on the healing of cutaneous wound on healthy and iron-deficient Wistar rats and their impact on fibroblastic activity during wound healing. *Lasers Med Sci* 2013;28:799-806.

17. Firat ET, Dağ A, Günay A, et al. The effect of low-level laser therapy on the healing of hard palate mucosa and the oxidative stress status of rats. *J Oral Pathol Med* 2014;43:103-110.

18. de Sousa AP, Paraguassu GM, Silveira NT, et al. Laser and LED phototherapies on angiogenesis. *Lasers Med Sci* 2013;28:981-987.

19. Chang PC, Chien LY, Ye Y, Kao MJ. Irradiation by light-emitting diode light as an adjunct to facilitate healing of experimental periodontitis in vivo. *J Periodontal Res* 2013;48:135-143.

20. Cory G. Scratch-wound assay. *Methods in molecular biology* 2011;769:25-30.

21. Chang PC, Tsai SC, Jheng YH, Lin YF, Chen CC. Soft-tissue wound healing by anti-advanced glycation end-products agents. *J Dent Res* 2014;93:388-393.

22. Ko JH, Kim PS, Zhao Y, Hong SJ, Mustoe TA. HMG-CoA reductase inhibitors (statins) reduce hypertrophic scar formation in a rabbit ear wounding model. *Plast Reconstr Surg* 2012;129:252e-261e.

23. Favaro-Pipi E, Ribeiro DA, Ribeiro JU, et al. Low-level laser therapy induces differential expression of osteogenic genes during bone repair in rats. *Photomed Laser Surg* 2011;29:311-317.

24. Kudo A. Periostin in fibrillogenesis for tissue regeneration: periostin actions inside and outside the cell. *Cell Mol Life Sci* 2011;68:3201-3207.

25. Kahnberg KE, Thilander H. Healing of experimental excisional wounds in the rat palate. (I) Histological study of the interphase in wound healing after sharp dissection. *Int J Oral Surg* 1982;11:44-51.

26. Medrado AR, Pugliese LS, Reis SR, Andrade ZA. Influence of low level laser therapy on wound healing and its biological action upon myofibroblasts. *Lasers Surg Med* 2003;32:239-244.

27. Walsh LJ. The current status of laser applications in dentistry. *Aust Dent J* 2003;48:146-155; quiz 198.

28. Medrado AP, Soares AP, Santos ET, Reis SR, Andrade ZA. Influence of laser photobiomodulation upon connective tissue remodeling during wound healing. *J Photochem Photobiol B* 2008;92:144-152.

29. Saygun I, Karacay S, Serdar M, Ural AU, Sencimen M, Kurtis B. Effects of laser irradiation on the release of basic fibroblast growth factor (bFGF), insulin like growth factor-1 (IGF-1), and receptor of IGF-1 (IGFBP3) from gingival fibroblasts. *Lasers Med Sci* 2008;23:211-215.

30. de Sousa AP, Paraguassú GM, Silveira NT, et al. Laser and LED phototherapies on angiogenesis. *Lasers Med Sci* 2013;28:981-987.

31. Hawkins DH, Abrahamse H. The role of laser fluence in cell viability, proliferation, and membrane integrity of wounded human skin fibroblasts following helium-neon laser irradiation. *Lasers Surg Med* 2006;38:74-83.

32. Aleksic V, Aoki A, Iwasaki K, et al. Low-level Er:YAG laser irradiation enhances osteoblast proliferation through activation of MAPK/ERK. *Lasers Med Sci* 2010;25:559-569.

33. Sacono NT, Costa CA, Bagnato VS, Abreu-e-Lima FC. Light-emitting diode therapy in chemotherapy-induced mucositis. *Lasers Surg Med* 2008;40:625-633.

34. Fujimoto K, Kiyosaki T, Mitsui N, et al. Low-intensity laser irradiation stimulates mineralization via increased BMPs in MC3T3-E1 cells. *Lasers Surg Med* 2010;42:519-526.

35. Pyo SJ, Song WW, Kim IR, et al. Low-level laser therapy induces the expressions of BMP-2, osteocalcin, and TGF-beta1 in hypoxic-cultured human osteoblasts. *Lasers Med Sci* 2013;28:543-550.

36. Greiling D, Clark RA. Fibronectin provides a conduit for fibroblast transmigration from collagenous stroma into fibrin clot provisional matrix. *J Cell Sci* 1997;110 (Pt 7):861-870.

37. Altay MA, Tasar F, Tosun E, Kan B. Low-level laser therapy supported surgical treatment of bisphosphonate related osteonecrosis of jaws: a retrospective analysis of 11 cases. *Photomed Laser Surg* 2014;32:468-475.

38. Vescovi P, Meleti M, Merigo E, et al. Case series of 589 tooth extractions in patients under bisphosphonates therapy. Proposal of a clinical protocol supported by Nd:YAG low-level laser therapy. *Med Oral Patol Oral Cir Bucal* 2013;18:e680-685.

39. Redlich K, Smolen JS. Inflammatory bone loss: pathogenesis and therapeutic intervention. *Nat Rev Drug Discov* 2012;11:234-250.

40. Sorci G, Riuzzi F, Giambanco I, Donato R. RAGE in tissue homeostasis, repair and regeneration. *Biochimica et biophysica acta* 2013;1833:101-109.

Corresponding author: Po-Chun Chang DDS, PhD, Graduate Institute of Clinical Dentistry, School of Dentistry, National Taiwan University, 1 Chang-Te St, Taipei 100, Taiwan, Phone: +886-2-2312-3456 extension 67709, Fax: +886-2-2383-1346, E-mail: changpc@ntu.edu.tw

Submitted October 10, 2014; accepted for publication December 5, 2014.

Figure 1.

Gingival Fibroblasts under LED light Irradiations. ***(A)*** *Cellular viability was evaluated by the MTS Assay at the absorbance wavelength of 490 nm.* ***(B)*** *Cytotoxicity by the LDH Assay. Data are presented as the cytotoxicity relative to the specimens without LED light irradiation (set as zero) at the same time point.* ***(C)*** *Cell migration by the distance of cells traveled from the edges of the wound relative to the baseline. (Compare to non-LED irradiated specimens at the same time point: *$p<0.05$, †$p<0.01$, ‡$p<0.001$)*

Figure 2.

Descriptive Histology of the specimens with LED light irradiation at days 7-28. Magnification: 100x. Scale bar: 100 μm. ***(A)*** *A specimen of Ctrl group at day 7.* ***(B)*** *A specimen of LD group at day 7.* ***(C)*** *A specimen of HD group at day 7.* ***(D)*** *A specimen of Ctrl group at day 14.* ***(E)*** *A specimen of LD group at day 14.* ***(F)*** *A specimen of HD group at day 14* ***(G)*** *A specimen of Ctrl group at day 28.* ***(H)*** *A specimen of LD group at day 28.* ***(I)*** *A specimen of HD group at day 28. Asterisks indicate the sequestrum.*

Figure 3.

Histochemical and immunohistochemical assessments of the specimens with the LED light irradiation. Magnification: 200x. Scale bar: 100 μm. ***(A-D)*** *Masson's Trichrome-stained specimens.* ***(A)*** *A specimen of Ctrl group at day 7.* ***(B)*** *A specimen of Ctrl group at day 14.* ***(C)*** *A specimen of LD group at day 14.* ***(D)*** *A specimen of LD group at day 28.* ***(E-I)*** *Specimens stained with anti-TNF-α antibody.* ***(E)*** *A specimen of Ctrl group at day 7.* ***(F)*** *A specimen of LD group at day 7.* ***(G)*** *A specimen of Ctrl group at day 14.* ***(H)*** *A specimen of LD group at day 14.* ***(I)*** *A specimen of Ctrl group at day 28.*

Figure 4.

Quantitative Histological Assessments. ***(A)*** *The extent of wound closure, 40x.* ***(B)*** *The extent of re-epithelization, 100x.* ***(C)*** *The scar elevation index (SEI), 40x.* ***(D)*** *The fraction of inflammatory cells/total cells in the wound, 400x.* ***(E)*** *The fraction of collagen deposition/lamina propria in the wound, 100x.* ***(F)*** *The fraction of TNF-α-positive area/lamina propria in the wound, 100x. (HD or LD group compare to control group at the same time point: *$p<0.05$, †$p<0.01$; HD group compare to LD group at the same time point: ‡$p<0.05$)*

Figure 5.

Gene Expression in the palatal wound under LED light irradiation. ***(A)*** *Heme oxygenase-1 (HO-1).* ***(B)*** *Tumor necrosis factor-alpha (TNF-α).* ***(C)*** *Receptor for advanced glycation end-products (RAGE).* ***(D)*** *Vascular-endothelial growth factor (VEGF).* ***(E)*** *Periostin.* ***(F)*** *Type I collagen.* ***(G)*** *Fibronectin. (HD or LD group compare to control group at the same time point: $^{*}p<0.05$, $^{\dagger}p<0.01$, $^{\ddagger}p<0.001$; HD group compare to LD group at the same time point: $^{\S}p<0.001$)*

‖ JETTS Tech Co., New Taipei City, Taiwan

¶ CellTier® 96 AQueous One Solution Cell Proliferation Assay, Promega, Madison, WI, USA

Cytotoxicity Detection Kitplus, LDH, Roche, London, UK

** AxioCam ERc5s, Carl Zeiss Microscopy GmbH, Munich, Germany

†† Cell & Tissue Staining Kit, R&D systems, Minneapolis, MN, USA

‡‡ Polyclonal anti-TNF-antibody, Abcam PLC, Cambridge, UK

§§ AxioCam ERc5s, Carl Zeiss Microscopy GmbH, Munich, Germany

‖ ‖ Image-Pro Plus software Media Cybernetics Inc., Rockville, MD, USA

¶¶ iScript cDNA Synthesis Kit, Bio-Rad Laboratories

StepOnePlus, Applied Biosystems

*** Applied Biosystems

 DOI: 10.1902/jop.2015.140580

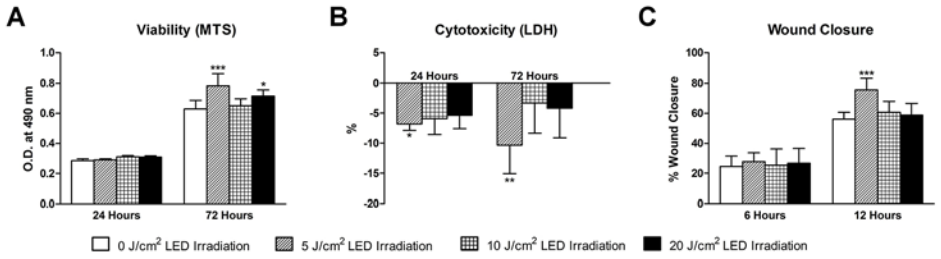

 DOI: 10.1902/jop.2015.140580

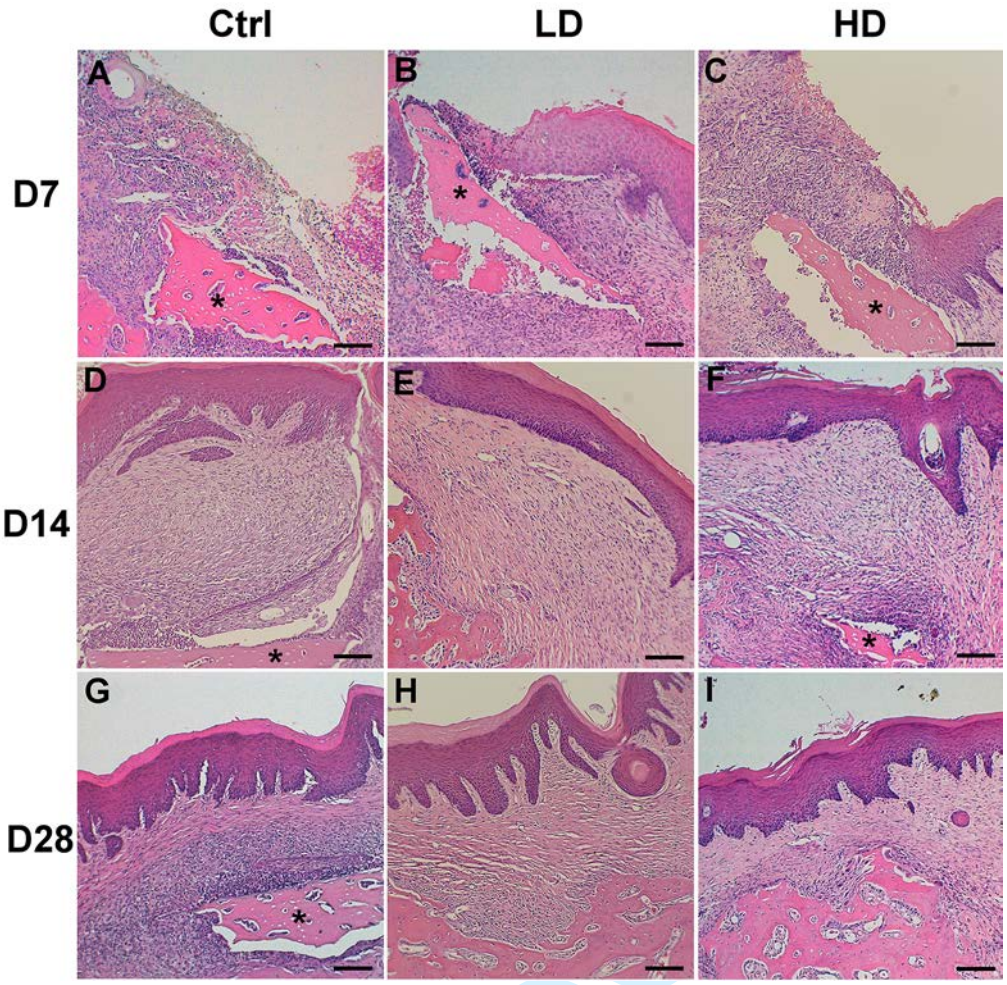

 DOI: 10.1902/jop.2015.140580

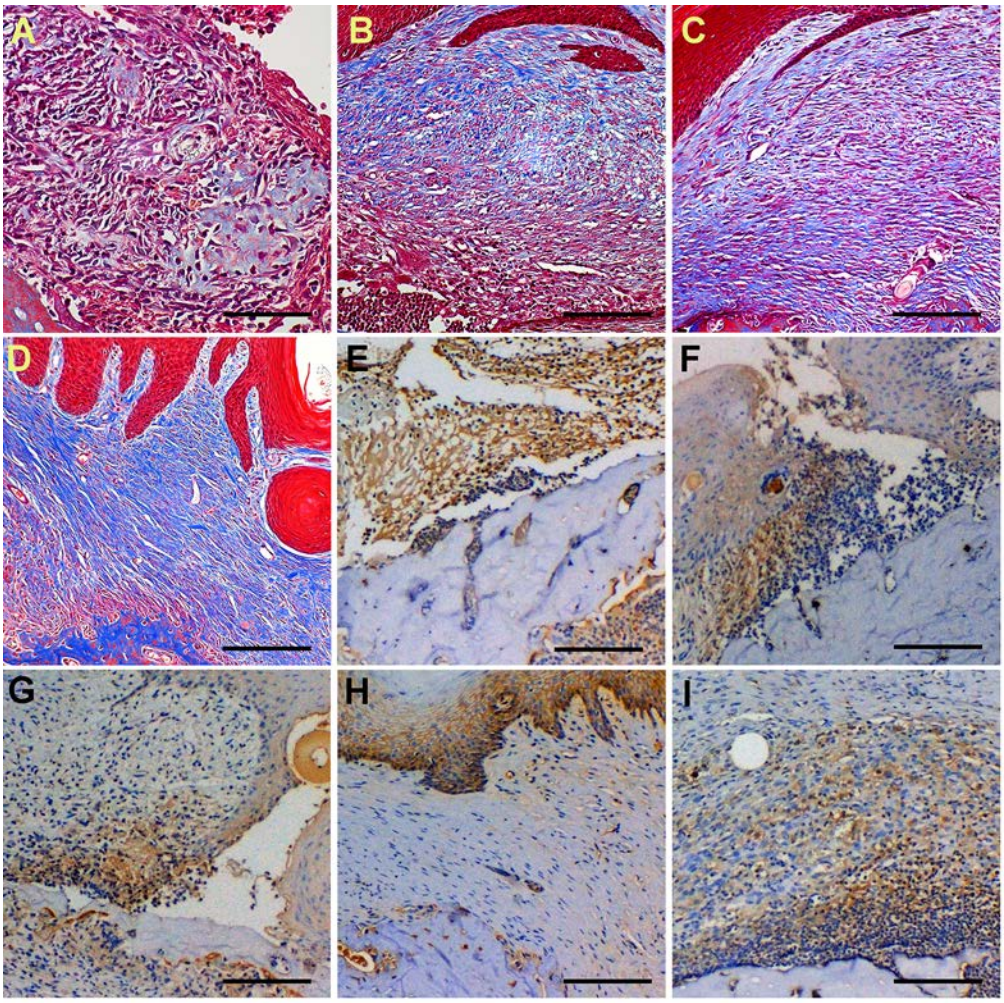

 DOI: 10.1902/jop.2015.140580

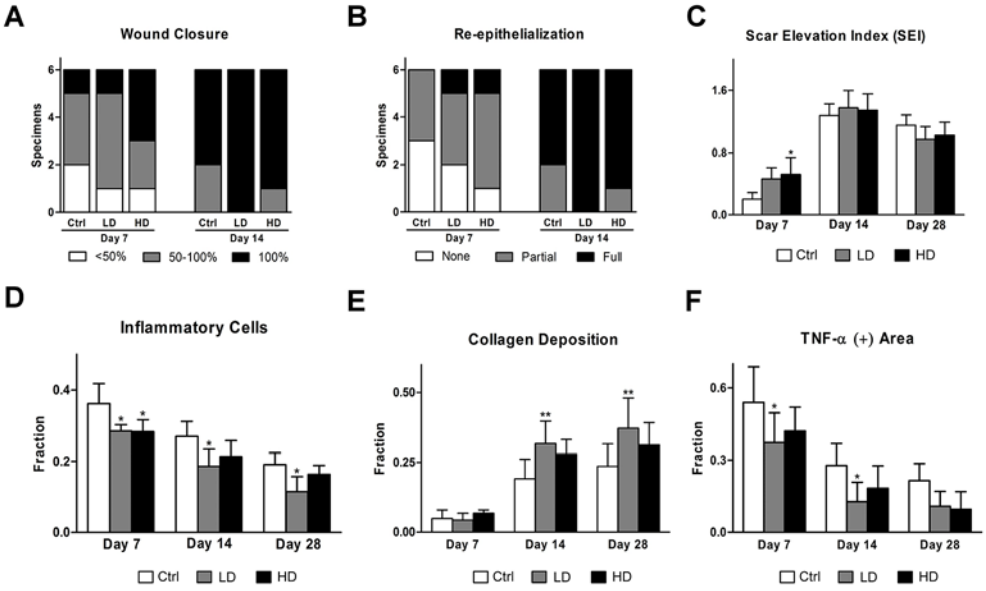

 DOI: 10.1902/jop.2015.140580